

# Interaction of a relativistic electron beam with a dense plasma

V. A. Kiselev, A. K. Berezin, and Ya. B. Fainberg

Physico-technical Institute, Ukrainian Academy of Sciences

(Submitted December 10, 1975)

Zh. Eksp. Teor. Fiz. 71, 193-202 (July 1976)

Results are presented of an experimental investigation of the efficiency of interaction between a monoenergetic relativistic electron beam and a dense plasma ( $n_p \sim 10^{15} - 10^{17} \text{ cm}^{-3}$ ). It is shown that the efficiency of interaction between a monoenergetic, low-divergence beam and a plasma does not decrease with increasing plasma density. Localized electromagnetic radiation from the interaction region with a wavelength  $\lambda \sim 1 \text{ mm}$  and soft localized x rays are observed. A spatial correlation is found between the x-ray and microwave production region and the region of decrease of the plasma density.

PACS numbers: 52.40.Mj

## INTRODUCTION

One of the most important problems of beam-plasma interaction is how to increase the efficiency of the interaction of relativistic electron beams with a dense plasma. This interaction can be used, in particular, to heat a dense plasma to thermonuclear temperatures and to produce beam-plasma generators for the millimeter and submillimeter bands.<sup>[1-3]</sup>

In a large number of experiments, the efficiency of the interaction of relativistic electron beams with a plasma has decreased with increasing plasma density.<sup>[4-6]</sup> These experiments, however, were performed using large-angular-divergence relativistic beams with a large energy scatter. In our experiments we used well collimated and highly monoenergetic relativistic beams with small divergence angle  $\Delta\theta \lesssim 10'$ . Under these conditions, as is well known, the relativistic beams and the plasma interact strongly, so that the instability has a hydrodynamic character.<sup>[7]</sup>

With increasing energy and angle scatter, the instability becomes kinetic and the instability growth rate decreases strongly<sup>[8]</sup>:

$$\delta \sim \omega_p \frac{n_b}{n_p} \frac{1}{\gamma} \frac{1}{(\Delta\theta)^2}, \quad (1)$$

i. e.,  $\delta \sim n_p^{-1/2}$ . Here  $\omega_p$  is the plasma natural frequency,  $n_b$  is the beam density,  $n_p$  is the plasma density, and  $\gamma = (1 - v^2/c^2)^{-1/2}$  is the relativistic factor. Thus, the growth rate decreases with increasing plasma density, so that the interaction efficiency also decreases.

In the case of a monoenergetic beam with a small angle scatter interacting with a plasma, hydrodynamic instability can develop, with a growth rate<sup>[9]</sup>

$$\delta \sim \omega_p \left( \frac{n_b}{n_p} \right)^{1/2} \frac{1}{\gamma}, \quad (2)$$

i. e.,  $\delta \sim n_p^{1/2}$  increases with increasing plasma density.

Our present study has demonstrated experimentally that the efficiency of the interaction of a well-collimated relativistic electron beam ( $\Delta\theta \lesssim 10'$ ) with a plasma of density  $10^{15}$  to  $10^{17} \text{ cm}^{-3}$  does not decrease. The

interaction efficiency is essentially influenced by the beam current and by the width of the beam-electron energy distribution function.

## 1. EXPERIMENTAL SETUP

The setup used with the experiments is illustrated in Fig. 1. The electron beam, obtained from an electron accelerator, had the following parameters: energy 2 MeV, beam current 1 A, pulse duration 2  $\mu\text{sec}$ , beam diameter 1 cm. To obtain a pulse configuration of high density ( $n_p \sim 10^{15} - 10^{17} \text{ cm}^{-3}$ ) we used a coaxial plasma gun operating in the "plasma focus" regime.<sup>[10,11]</sup> Inasmuch as oscillations with small wavelengths (on the order of a millimeter or less), are excited in the plasma at such densities, and the geometrical dimensions of the plasma exceed 10 cm in length and several centimeters in diameter, the effects of beam modulation ( $f_M = 2800 \text{ MHz}$ ), reported in<sup>[7]</sup>, do not play any role in this case, since  $\omega_M \ll \omega_p$ . We have therefore investigated in our experiments the interaction of an unmodulated relativistic electron beam with an unbounded plasma.

The electron beam, focused by a long-focus magnetic lens at the exit from the accelerator, was guided with the aid of a corrector, through an aperture in the internal electrode of the gun, into the interaction region, which comprised a glass tube 10 cm in diameter and 50 cm long. There was no external magnetic field. The density of the plasma with which the electron beam interacted depended on the delay between the start of the formation of the plasmoid and the triggering of the electron accelerator. The plasma variation in time and in space, with and without passage of the beam through the

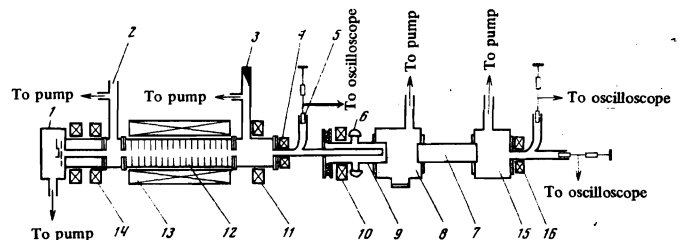


FIG. 1.

plasma, was measured by determining the hydrogen  $H_\beta$  and  $H_\gamma$  line broadening due to the Stark effect, and also with the aid of a laser interferometer of the Michelson type. The radiation source in the interferometer was a laser operating at  $10.6 \mu$  wavelength. The laser output power was 5–10 W. The detector was a GeAu photoresistor at liquid-nitrogen temperature. The plasma density was measured with the interferometer accurate to 10%.

The current of the relativistic electron beam passing through the plasma was registered with a Faraday cup. Magnetic analyzers located at the exit from the accelerator and past the interaction chamber were used to plot the beam electron energy distribution functions before and after passage through the plasma. The electromagnetic radiation from a plasma interacting with a relativistic beam was registered with the aid of a pyroelectric pickup with a cut-off 2-millimeter wave guide at the input and calibrated germanium crystal detectors with horn antennas, tuned to receive radiation in the  $\sim 1$  mm wave band. The pyroelectric pickup has a very high inertia when it comes to registering pulsed electromagnetic radiation, but it can be used to estimate the radiation power, since the voltage-power characteristic as a function of the pulse duration is of the form<sup>[12]</sup>

$$U/P = 0.02T, \quad (3)$$

where  $U$  is the signal amplitude in volts,  $P$  is the radiation power in watts, and  $T$  is the pulse duration in microseconds.

The soft x radiation from the plasma was studied with the aid of a pinpoint camera and a semiconducting x-ray pickup with angular aperture  $\alpha = 0.15^\circ$ , which could be moved both along the system axis and along the diameter of the interaction chamber.

## 2. RESULTS OF EXPERIMENTAL INVESTIGATION OF THE INTERACTION OF A RELATIVISTIC BEAM WITH A DENSE PLASMA

Figure 2a shows the energy spectra of the beam before and after its passage through a plasma of density  $n_p \lesssim 10^{16} \text{ cm}^{-3}$ . It is seen from the figure that the beam energy loss in this case reaches 20% of the initial value, i.e., the same as at a density  $n_p \sim 10^{11} \text{ cm}^{-3}$ ,<sup>[7]</sup> even though the beam-modulation effects do not play any

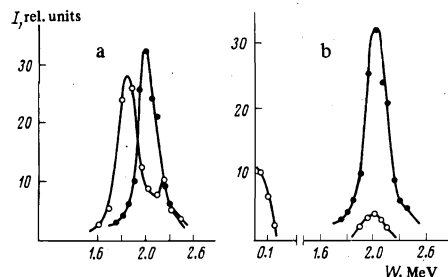


FIG. 2. Energy spectra of beam electron: ●—without plasma, ○—after passing through plasma. a—plasma power  $n_p \lesssim 10^{16} \text{ cm}^{-3}$ , b— $n_p \sim 4 \cdot 10^{16} \text{ cm}^{-3}$ .

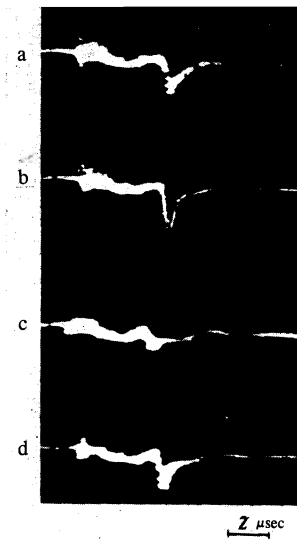


FIG. 3. Oscillograms of electromagnetic radiation signals ( $\lambda \sim 1$  mm): a— $n_p < 5 \cdot 10^{15} \text{ cm}^{-3}$ ; b— $n_p \sim 5 \cdot 10^{15} \text{ cm}^{-3}$ ; c— $n_p \sim 5 \cdot 10^{16} \text{ cm}^{-3}$ ; d— $n_p \sim 5 \cdot 10^{15} \text{ cm}^{-3}$ .

role in this case ( $\omega_M \ll \omega_p$ ).

When the plasma density was increased to  $n_p \sim (4-6) \times 10^{16} \text{ cm}^{-3}$ , the beam current registered by the Faraday cup decreased strongly,<sup>[13]</sup> and electrons of energy  $\sim 100$  kV appeared in the energy spectrum of the electron beam (Fig. 2b), i.e., the electron-beam energy loss reached  $\sim 90\%$ .

Measurements with a pyroelectric pickup and crystal detectors have revealed the presence of electromagnetic radiation of wavelength  $\sim 1$  mm from a plasma interacting with a relativistic beam. The electromagnetic-radiation signal oscillograms obtained with calibrated semiconductor detectors are shown in Fig. 3. It is seen from this figure that the signal amplitude is maximal at a plasma density  $n_p \sim 5 \times 10^{15} \text{ cm}^{-3}$ . With increasing (as well as decreasing) plasma density, the signal amplitudes decrease. The obvious reason is the decrease of the interaction efficiency (with decreasing plasma density) and the loss of the detector sensitivity as the radiation wavelength decreases (with increasing plasma density).

The oscillograms of Figs. 3a, 3b, and 3c refer to the case when the horn antenna of the detector is perpendicular to the system axis in the region where the plasma is produced. Figure 3d shows the radiation signal when the horn antenna makes an angle of  $30^\circ$  with the initial position relative to the system-output direction, and the plasma density is  $\sim 5 \times 10^{15} \text{ cm}^{-3}$ . The decrease of the signal in this case indicates that the electromagnetic radiation is localized in the region of the plasma formation at the instant when the electron beam passes through it.

It was noted in the course of the experiments that when a beam interacts with a plasma of density  $n_p \sim 5 \times 10^{15} \text{ cm}^{-3}$  and higher, soft x rays are observed to be emitted from the region of the plasma formation; these x rays were not registered in the absence of the beam. The measurements have shown that besides the high-energy ( $\sim 2$  MeV) sharply-directional x radiation, which is obviously due to the bremsstrahlung of the electrons

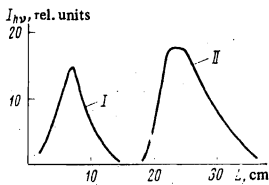


FIG. 4. Distribution of x rays along the interaction chamber. I—first zone, II—second zone.

of the relativistic beam, there are also two zones of softer x radiation, which is produced only when the beam passes through the plasma (Fig. 4) and is isotropic in character.

The first zone is located 4–8 cm away from the end face of the plasma gun, i. e., in the plasma-formation region. From an x-ray photograph of this zone, obtained with a pinpoint camera whose optical axis was perpendicular to the system axis, it is seen that the first zone has a diameter of ~3 cm and length 4–5 cm, i. e., the geometrical dimensions are much less than those of the plasma formation (Fig. 5). The maximum x-ray energy from this zone is ~15 keV. The geometric dimensions of this zone decreased with increasing plasma density and increased with decreasing plasma density.

The intensity of the referred-to x radiation depends strongly on the width of the beam electron energy distribution function. When the width of the electron energy spectrum increases from 10 to 80%, the radiation intensity decreases by more than one order of magnitude (Fig. 6a). In addition, the intensity of this radiation decreases with decreasing electron-beam current. This relation is shown in Fig. 6b for the case when the width of the energy spectrum of the beam electrons is 10%. It should be noted that with increasing width of the electron energy distribution function and with decreasing beam current, the beam energy losses also decrease as the beam interacts with the plasma. At a beam current  $I \lesssim 10$  mA the beam passes through the plasma with practically no energy loss.

The second x-ray zone (Fig. 4, zone II) is located 30–60 cm away from the end. The radiation energy for this zone is ~100 keV and the diameter of the radiation region coincides with the diameter of the interaction chamber. This gives grounds for assuming that this x radiation is due to electrons that lose their energy in collective interaction with the dense plasma and strike the chamber wall as a result of scattering by the dense plasma. Electrons with this energy were registered also with a magnetic analyzer (Fig. 2b). With increasing width of the energy spectrum of the beam electrons, the second x-ray zone broadens and the energy increases, thus indicating a decrease in the effectiveness of the collective interaction of the relativistic beam with

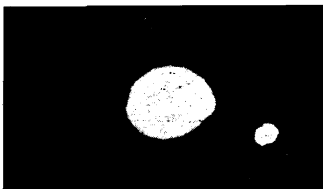


FIG. 5. X-ray pinpoint photograph of first zone.

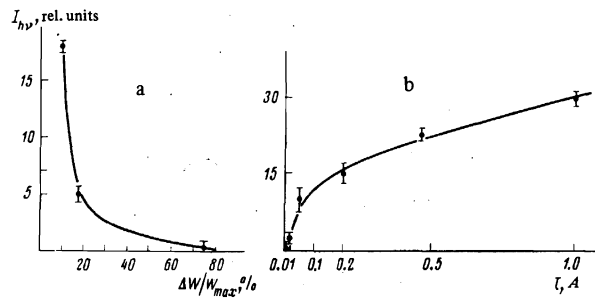


FIG. 6. Intensity of the x radiation of the first zone as a function of the beam-electron energy spectrum (a) and intensity of the soft x rays as a function of the beam current (b).

the dense plasma.

The large energy lost by a relativistic beam interacting with a dense plasma, together with the appearance of localized x radiation, offers evidence of the possible occurrence of strong high-frequency electric fields, in which the plasma electrons can acquire energy. In this case there should be observed in the interaction region a decrease in the energy of the plasma that is being crowded out by the fields.<sup>[14,15]</sup> Figure 7 shows an interference pattern of the plasma without the beam (a) and an interference pattern of the plasma through which an electron beam passes (b); both patterns were obtained with a laser interferometer. The same figure shows oscillograms of the x-ray signal (c) and the beam current loss (d, e). Figure 7f shows the time dependence of the plasma density without the beam and with a beam passing through the plasma, as determined from the interference patterns of Figs. 7a and 7b. The calculations show that at the instant of the passage of the beam the plasma density in the region of the localization of the x rays and the microwaves decreases to  $n_p \sim 2 \times 10^{15} \text{ cm}^{-3}$  in comparison with the plasma density without the beam ( $n_p \sim 2 \times 10^{16} \text{ cm}^{-3}$ ). It should be noted that a laser interferometer measures the plasma density averaged over the plasmoid cross section. The estimated lowering of the plasma density in the x-ray localization region can therefore reach  $10^{14} \text{ cm}^{-3}$ . As

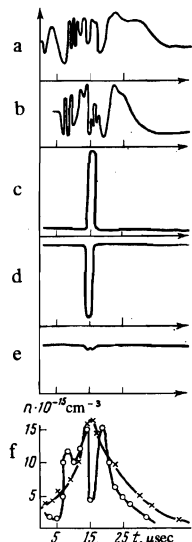


FIG. 7. a) Interference pattern of plasma without beam, b) interference pattern of plasma through which a beam passes, c) oscillogram of start of x-ray signal, d) current of beam without plasma, e) current of beam after passing through the plasma, f) time dependence of the plasma density; x—without beam, o—with beam.

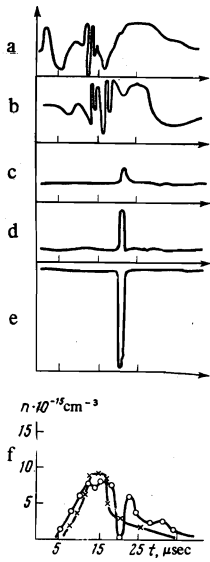


FIG. 8. a) Interference pattern of plasma without beam, b) interference pattern of plasma following passage of beam, c) oscillogram of microwave signal ( $\lambda \sim 1$  mm), d) oscillogram of x-ray signal, e) beam current after passage through plasma, f) time dependence of the plasma density:  $\times$ —without beam,  $\circ$ —with beam.

seen from the figure, the instant when the plasma density is lowered in the localization region corresponds to the instant when the x-ray signal is produced and the beam current is abruptly decreased.

With increasing time delay between the start of the formation of the plasmoid and the triggering of the electron accelerator, when the beam interacts with a plasma of lower density ( $n_p \sim 5 \times 10^{15}$  cm $^{-3}$ ), a decrease takes place both in the energy loss by the beam (Fig. 2b) and in the x-ray amplitude (Fig. 8). In this case electromagnetic radiation of wavelength  $\lambda \sim 1$  mm was observed to emerge from the interaction region.

No decrease of the plasma density was observed when the laser beam passed outside the x-ray and microwave regions.

### 3. DISCUSSION OF RESULTS

The experimental results show that the effectiveness of the collective interaction of a monoenergetic relativistic electron beam with a plasma increases with increasing plasma density. At the start of the interaction process, the collision frequency in the plasma in our experiments is high ( $n_p \sim 10^{16}$  cm $^{-3}$ ,  $T_e \sim 4$  eV,  $\nu \sim 1.4 \times 10^{11}$  sec $^{-1}$ ), and then decreases as the beam instability develops. Therefore at the initial instant there can develop a dissipative instability. For this instability to develop it is necessary to satisfy the condition (see<sup>[16]</sup>)

$$\frac{\Delta v}{v_0} \lesssim \frac{\delta}{\omega_p} \sim \left(\frac{n_b}{n_p}\right)^{1/2} \frac{1}{\gamma}. \quad (4)$$

At  $n_b \sim 5 \times 10^8$  cm $^{-3}$  and  $\gamma = 5$ , the condition for the development of dissipative instability is  $\Delta v/v_0 \lesssim 10^{-3}$ . At the same time, as follows from<sup>[17]</sup>, the scatter of the beam electrons over the longitudinal velocities is determined by the width  $\Delta E/E$  of the energy spectrum and by the initial angle spread  $\Delta\theta$  of the beam particles

$$\frac{\Delta v}{v_0} \sim \frac{\Delta E}{E\gamma^2} + (\Delta\theta)^2. \quad (5)$$

In our experiments we have  $\Delta E/E \sim 8\%$ ,  $\Delta\theta \sim 2.5 \times 10^{-3}$ , i. e.,  $\Delta v/v_0 \sim 3 \times 10^{-3}$ , from which it follows that dissipative instability can develop under our conditions.

The spatial growth rate of such an instability<sup>[18]</sup>

$$\kappa_D \sim \frac{\omega_b}{v_0} \frac{1}{\gamma^{1/2}} \left(\frac{\omega_p}{v}\right)^{1/2} \quad (6)$$

increases with increasing plasma density ( $\kappa_D \propto n_p^{1/4}$ ) and amounts to  $\kappa_D \approx 3 \times 10^{-1}$  cm $^{-1}$  for the parameters indicated above. Consequently, the relaxational length of a relativistic electron beam in such a plasma amounts to several centimeters.

When dissipative instability develops, the plasma temperature increases,<sup>[16]</sup> and this can lead to a decrease in the collision frequency ( $\nu \sim 1/T_e^{3/2}$ ), such that collisionless instability ( $\nu < \delta$ ) can develop. For example, we have  $\nu \sim 10^{18}$  sec $^{-1}$  already at  $T_e \sim 100$  eV and  $n_p \sim 10^{16}$  cm $^{-3}$ . The spatial growth rate of this instability<sup>[8]</sup>

$$\kappa_B = \left(\frac{n_b}{n_p} \frac{v_0}{v_g}\right)^{1/2} \frac{\omega_p}{v_0 \gamma} \quad (7)$$

also increases with increasing plasma density ( $\kappa_B \propto n_p^{1/8}$ ). Since there is no external magnetic field in our experiments, it follows that  $v_g \sim 3v_{Te}^2/v_0$ . Here  $v_0 \approx c$  is the beam velocity,  $v_g$  is the group velocity, and  $v_{Te}$  is the plasma-electron thermal velocity. At the parameters indicated above we have  $\kappa_B \sim 4$  cm $^{-1}$ , i. e., the beam relaxation rate is in this case of the order of a centimeter.

We propose therefore the following picture of the interaction of a monochromatic relativistic electron beam with a dense plasma: dissipative instability develops first ( $\nu > \delta$ ) and leads to an increase of the plasma temperature, and as a consequence to a decrease in the collision frequency ( $\nu < \delta$ ). This is followed by development of a collisionless instability with a small relaxation length and with large beam-energy losses to excitation of oscillations. The collective interaction of the relativistic beam with the dense plasma is manifested by the observed electromagnetic radiation of wavelength  $\lambda \sim 1$  mm, localized in the interaction region.<sup>1)</sup> This is confirmed also by the presence of localization of soft x rays in the interaction region. The electrons that cause this x radiation apparently acquire energy in the high-frequency electric fields excited by the electron beam in the dense plasma. This is evidenced by the spatial and temporal correlations which were established here between the onset of the regions of the intense x-ray and microwave radiation, and also by the appreciable decrease of the plasma density in the region where the x rays and microwave radiation are localized. The formation of a "hole" (a region with decreased density) in the plasma coincides also in time with the instant of the appearance of localized x-ray and microwave regions. The decrease of the plasma density is obviously due to the action of the pressure forces of the HF field, as was the case in experiments with nonrelativistic beams with a tenuous plasma.<sup>[19,20]</sup>

The possibility of crowding out of a plasma by an

electric HF field can be qualitatively estimated in our case from the condition<sup>[8]</sup>

$$\frac{E^2}{4\pi} = \alpha_T \frac{v_0}{v_g} n_b m v_0^2 \gamma, \quad \alpha_T \approx \left( \frac{n_b}{n_p} \frac{v_0}{v_g} \right)^{1/2} \gamma < 1. \quad (8)$$

If the pressure of the electric HF field is equal to the thermal pressure of the plasma in the region where the density is decreased we have

$$E^2/4\pi n_p T \sim \delta n_p/n_p \sim 1 \quad (9)$$

for the initial conditions ( $n_p \sim 10^{16} \text{ cm}^{-3}$ ,  $n_b = 5 \times 10^8 \text{ cm}^{-3}$ ,  $v_g \sim 10^8 \text{ cm/sec}$ ) we have  $\alpha_T = 0.55$ . It follows then from (8) and (9) that in the stationary case, at a density  $n_p \sim 10^{14} \text{ cm}^{-3}$ , the plasma electrons can acquire an energy up to 200 keV if the entire beam energy were to go into the development of HF oscillations. In our experiments we registered radiation with maximum energy up to 15 keV.

The abrupt decrease of the beam current following interaction with a plasma of density  $n_p > 10^{16} \text{ cm}^{-3}$  (Fig. 7) is obviously due to the scattering of the beam electrons, which lose energy as a result of collective interaction with the plasma, from the interaction-chamber walls by elastic scattering with the dense plasma. This is evidenced by the second zone of x rays with energy  $E_{hv} \geq 100 \text{ keV}$  emitted from the walls of the interaction chamber.

Thus, our experimental investigations of the interaction of a relativistic electron beam with a dense plasma have shown that the efficiency of collective interactions of a monoenergetic beam does not decrease with increasing plasma density. These interactions, which lead to a strong decrease of the beam relaxation length in the plasma, are accompanied by excitation of millimeter waves and localized x rays. The observed temporal and spatial correlations of the zones in which the plasma density decreases, the localized x-ray zone and the microwave radiation zone, point to the presence of a localized region of strong high-frequency fields in which the plasma electrons acquire energy.

We have established a connection between the observed phenomenon, the degree to which the beam is monoenergetic, and the distribution function of the electrons of the relativistic beam with respect to energy. This connection is of decisive significance for collective interactions of such a beam with a dense plasma.

<sup>1</sup>The measurements were performed with a pyroelectric pickup of known sensitivity and angular aperture. The total power of the electromagnetic radiation was calculated by integrating over the angle and the length of the interaction region.

<sup>1</sup>Ya. B. Faĭnberg, *At. Energ.* **11**, 313 (1961).

<sup>2</sup>Ya. B. Faĭnberg and V. D. Shapiro, in: *Vzaimodeĭstvie zaryazhennykh chastits s plazmoy* (Interactions of Charged Particles with Plasma), Kiev, Naukova Dumka, 1965, p. 92.

<sup>3</sup>Ya. B. Faĭnberg, V. D. Shapiro, and V. I. Shevchenko, *Zh. Eksp. Teor. Fiz.* **57**, 966 (1969) [*Sov. Phys. JETP* **30**, 528 (1970)].

<sup>4</sup>A. G. Altyntsev, A. P. Es'kov, O. A. Zolotovskii, V. I. Koroteev, R. Kh. Kurtmullaev, V. A. Masalov, and V. N. Semenov, *Pis'ma Zh. Eksp. Teor. Fiz.* **13**, 197 (1971) [*JETP Lett.* **13**, 139 (1971)].

<sup>5</sup>C. A. Kapetanakis and D. A. Hammer, *Appl. Phys. Lett.* **23**, 17 (1973).

<sup>6</sup>Yu. I. Abrashitov, V. S. Koĭdan, V. V. Konyukhov, V. I. Logunov, V. P. Luk'yanov, K. I. Mekler, and D. D. Ryutov, *Zh. Eksp. Teor. Fiz.* **66**, 1324 (1974) [*Sov. Phys. JETP* **39**, 647 (1974)].

<sup>7</sup>A. K. Berezin, Ya. B. Faĭnberg, L. I. Bolotin, A. M. Egorov, V. A. Kiselev, V. A. Buts, V. I. Kurilko, and A. P. Tolstoluzhskii, *Zh. Eksp. Teor. Fiz.* **63**, 861 (1972) [*Sov. Phys. JETP* **36**, 453 (1973)].

<sup>8</sup>Ya. B. Faĭnberg and V. D. Shapiro, *Zh. Eksp. Teor. Fiz.* **47**, 1389 (1964) [*Sov. Phys. JETP* **20**, 937 (1965)].

<sup>9</sup>K. M. Watson, S. A. Bludman, and M. N. Rosenbluth, *Phys. Fluids* **3**, 741 (1960).

<sup>10</sup>A. I. Morozov, *Zh. Tekh. Fiz.* **37**, 2147 (1967) [*Sov. Phys. Tech. Phys.* **12**, 1580 (1968)].

<sup>11</sup>I. M. Zolototrubov, I. P. Skoblik, and Yu. M. Novikov, *Zh. Tekh. Fiz.* **43**, 281 (1973) [*Sov. Phys. Tech. Phys.* **18**, 184 (1973)].

<sup>12</sup>A. N. Akhiezer and V. I. Il'yashchenko, *Prib. Tekh. Ėksp.* No 5, 93 (1969).

<sup>13</sup>V. A. Kiselev, Ya. B. Faĭnberg, and A. K. Berezin, *Piz'ma Zh. Eksp. Teor. Fiz.* **20**, 603 (1974) [*JETP Lett.* **20**, 276 (1974)].

<sup>14</sup>V. E. Zakharov, *Zh. Eksp. Teor. Fiz.* **62**, 1745 (1972) [*Sov. Phys. JETP* **35**, 908 (1972)].

<sup>15</sup>A. A. Galeev, R. Z. Sagdeev, Yu. S. Sigov, V. D. Shapiro, and V. I. Shevchenko, *Fiz. Plasmy* **1**, 10 (1975) [*Sov. J. Plasma Phys.* **1**, 5 (1975)].

<sup>16</sup>A. A. Ivanov, V. V. Parail, and T. K. Soboleva, *Zh. Eksp. Teor. Fiz.* **63**, 1678 (1972) [*Sov. Phys. JETP* **36**, 887 (1973)].

<sup>17</sup>L. I. Rudakov, *Zh. Eksp. Teor. Fiz.* **59**, 2091 (1970) [*Sov. Phys. JETP* **32**, 1134 (1971)].

<sup>18</sup>V. U. Abramovich and V. I. Shevchenko, *Zh. Eksp. Teor. Fiz.* **62**, 1386 (1972) [*Sov. Phys. JETP* **35**, 730 (1972)].

<sup>19</sup>Bill Hong Quon, Preprint UCLA, Plasma Physics Group Report, PPG-176, 1974.

<sup>20</sup>H. C. Kim, R. L. Stenzel, and A. Y. Wong, Preprint UCLA, Plasma Physics Group Report, PPG-175, 1974.

Translated by J. G. Adashko